Chinese Chemical Letters 31 (2020) 1635–1639

Contents lists available at ScienceDirect

Chinese Chemical Letters

journal homepage: www.elsevier.com/locate/cclet

Communication

A nanocarrier based on poly(D,L-lactic-*co*-glycolic acid) for transporting Na^+ and Cl^- to induce apoptosis

Chen Ma, Yida Zhang, Zhijuan Jiao, Chunmeng Ma, Xiaoyan Liu, Haixia Zhang*

College of Chemistry and Chemical Engineering, Lanzhou University, Lanzhou 730000, China

ARTICLE INFO

Article history:
Received 17 July 2019
Received in revised form 6 September 2019
Accepted 9 September 2019
Available online 9 September 2019

Keywords:
Ions nanocarrier
Release fast
Transport ions
Inducing apoptosis
Caspase-dependent

ABSTRACT

Transmembrane anion transporters have attracted significant attention as therapeutic agents because of their potential to disrupt cellular ion homeostasis, in which, most of the synthetic anionic transporters are organic small molecules whose synthesis routes are usually complex and tedious, and the related biological research is also only in infancy. Hence, we synthesized a kind of chloride anion (Cl^-) and sodium cation (Na^+) nanocarrier based on poly(D,L-lactic-*co*-glycolic acid) (PLGA) which was coated with polydopamine (PDA) to provide target release factor. When the nanocarrier arrives in acidic environment such as lysosomes through endocytosis, Cl^- and Na^+ will be released fast from the nanocarrier resulting in imbalance of cell homeostasis for inducing apoptosis. Cell experiments show that the nanocarrier promotes apoptosis and leads to an increased concentration of reactive oxygen species. By exploring the concentration of cytochrome c in mitochondria and cytoplasm and the activities of key enzymes caspase-9 and caspase-3 in apoptosis process, it is proved that the apoptotic pathway is caspase-dependent. This novel strategy allows the research of anion transporter no longer limited to artificial synthesis of small molecular and provides a novel and effective direction to investigate ion homeostasis, ion transport and cancer treatment.

Anion transport has become one of the most important areas due to the important role in numerous biological and environmental processes [1–4]. It is an accepted notion that ions balance is involved in proliferation, migration and apoptosis of cancer cells [5–8]. The dysregulation of intracellular concentrations of ions, particularly, chloride [9,10], calcium and potassium ions [11], has been shown to correlate closely with the onset of apoptosis [12–15]. Therefore, devoting the study of physiological effects caused by ion imbalance at the cellular level is particularly significant in the field of ions transport. As one of the most important anions in physiological processes, Cl^- has critical role in a great variety of cellular processes, including neurotransmission, regulation of cytoplasmic, vesicular pH, cellular volume, and charge balance [16–18], which has become a hot spot in the field of ions transport. At present, the researches on the transport of Cl^- mainly focus on the artificial synthesis of small-molecule transporters based on the cotransport of H^+/Cl^- and Na^+/Cl^- [19–25]. Shins *et al.* have demonstrated two synthetic ion transporters which cotransport of Na^+/Cl^- into cells can induce apoptosis and death of cancer cells [26]. In 2017, they further synthesized a small molecular transporter which perturbs cellular Cl^- concentrations and promotes Na^+ influx into the cytosol can disrupt autophagy and induce apoptosis [27]. These studies have made great progress in the field of synthetic ion transporters. However, the synthesis of small molecule transporters is usually complex and these transporters are difficult to apply in biological system due to their biological incompatibility. Therefore, developing an applicable and biocompatible method to expand the application of ion transport in biological system is urgently needed.

Polymeric nanoparticles have become a hotspot for nanocarrier research in recent years due to its favorable biocompatibility and the ability of loading different types of substances [28–30]. Poly(D,L-lactic-*co*-glycolic acid) (PLGA) has been widely used as a carrier material for drug release owing to its excellent biocompatibility and biodegradability [31–34]. Cherng *et al.* loaded sodium bicarbonate ($NaHCO_3$) into the PLGA nanocarrier to achieve rapid release of doxorubicin under acidic conditions [35]. Mei *et al.* also used this method to achieve burst intracellular release of ciprofloxacin from PLGA hollow microspheres to induce cancer cell death [36]. These researches have confirmed that $NaHCO_3$ can assist the drug release quickly in the acidic environment. Polydopamine (PDA) has widely used as material surface modification since the PDA shells are not only stable enough but also provide target release. Liu *et al.* had reported a PDA-coated

* Corresponding author.
E-mail address: zhanghx@lzu.edu.cn (H. Zhang).

https://doi.org/10.1016/j.cclet.2019.09.010
1001-8417/

nanomaterial which can reach tumor site and release drugs successfully [37]. Shi *et al.* demonstrated that PDA film was pH sensitive [38], which would shed and break up in acidic conditions and the compounds loading by PDA film are easier to release in tumor tissue sites due to the acidic environment, thus achieving a targeted release effect [39,40]. The PDA "outerwear" of nanoparticles also has favorable hydrophilicity due to its sufficient hydroxyl and catechol structures, which can prevent the nanoparticles agglomeration to improve the stability [41,42]. Although polymers are used for loading various drugs, the research for loading ions is rare. Recently, Liu prepared a kind of sodium hyaluronate modified calcium peroxide nanoparticles and demonstrated the nanoparticles could cause calcium apoptosis in cancer cells and showed outstanding potential in cancer treatment [43].

Inspirited by the previous works, we designed a kind of NaCl and $NaHCO_3$ loaded PLGA nanocarrier (SPN@PDA) coated with polydopamine (PDA). The scheme of SPN@PDA and apoptosis pathway caused by the release of Na^+ and Cl^- in cells are shown in Fig. 1, in an acidic environment, Na^+ and Cl^- are released, and the ion equilibrium of the cells is destroyed. After that, cytochrome c is released from the mitochondria to the cytoplasm, activating caspase family to induce apoptosis ultimately.

Salt loaded PLGA nanoparticles (SPN) were easily prepared through improved water-in-oil-in-water (W/O/W) double emulsion method, and the detail was shown in supporting information. SPN was dispersed at pH 8.5 Tris-HCl buffer and coated with PDA by adding dopamine to the mixture to prepare SPN@PDA. As shown in Fig. S1 (Supporting information), TEM micrograph demonstrated SPN displayed a spherical and uniform morphology with a diameter of around 210 nm (Figs. S1a and c). After coated by PDA, the diameter of SPN@PDA became slightly larger and the PDA wrinkles served on the coverage (Figs. S1b and d). The peaks of PDA were observed in the FT-IR spectra (Fig. S1e), and the zeta potential was measured to investigate the surface modification and charge changes of SPN and SPN@PDA. Bare SPN showed a zeta potential of -67.5 ± 1.45 mV, after PDA coating, the zeta potential decreased to -105.0 ± 1.75 mV (Fig. S1f), which might be ascribed to the electronegativity of PDA. These results confirmed that the PDA was successfully modified on the surface of SPN. The control nanocarrier which only contains $NaHCO_3$ (PN@PDA) was also successfully prepared.

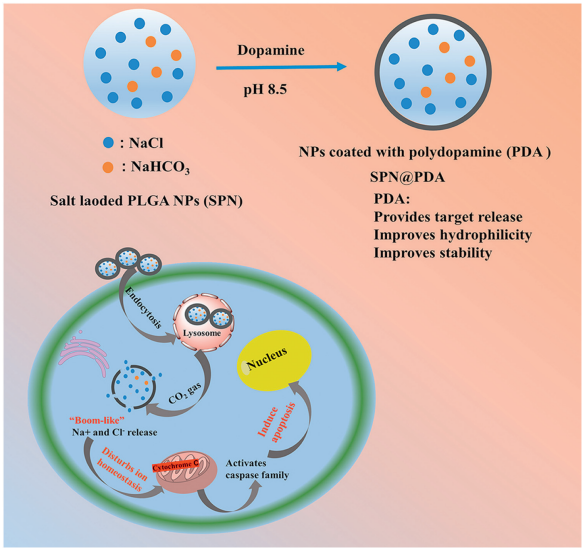

Fig. 1. The preparation of SPN@PDA and the mechanism of apoptosis through the release of Na^+ and Cl^-.

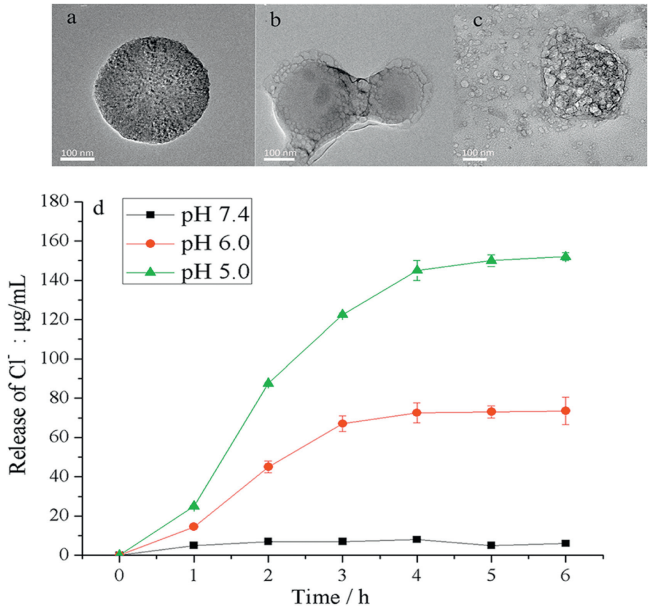

Fig. 2. Morphology of SPN@PDA at different pH. (a) pH 7.4 for 1 h; (b) pH 5.0 for 1 h; (c) pH 5.0 for 4 h; (d) the release rate at pH 7.4 (black), pH 6.0 (red) and pH 5.0 (green) at 37 °C, $n = 3$.

We verified the pH sensitivity of SPN@PDA by TEM. As illustrated in Fig. 2, when SPN@PDA was dispersed in PBS buffer at pH 7.4, it maintained a regular sphere (Fig. 2a). However, once SPN@PDA was dispersed in PBS buffer at pH 5, its shape began to collapse and bubbles appeared around it owing to CO_2 gas produced from the reaction between HCO_3^- and H^+ (Fig. 2b). When SPN@PDA was dispersed in an acidic environment for 4 h, the PDA shell was completely broken, and the encapsulated compounds inside were completely leaked (Fig. 2c). These results indicate that SPN@PDA can rapidly release loaded salts under acidic conditions. The loading capacity of SPN@PDA and release amount of Cl^- at different pH were determined by ion chromatography (IC). The loading amount of Cl^- in SPN@PDA determined by IC was 0.15 mg/mg. As shown in Fig. 2d, the concentration of released Cl^- from SPN@PDA at pH 7.4 (in the extracellular environment) was limited. However, once the nanocarrier reached the pH milieu of the early endosomes (pH 6.0, after 1 h) and the late endosomes/lysosomes (pH 5.0, after 1 h), the release of Cl^- increased significantly, and the release amount reached equilibrium after 4 h. These results prove that SPN@PDA has the ability of release ions rapidly under acidic conditions. Compared with the previous reports (16 h [35], 24 h [36], 8 h [43]), SPN@PDA has certain advantages in release rate.

To gain a better understanding of the effect of Cl^- and Na^+ released intracellularly, HeLa cells were incubated with dye-SPN@PDA (the material preparation is shown in supporting information) which contains a hydrophilic dye rhodamine B (RB) and a hydrophobic naphthalimide-based fluorophore (NA). The corresponding fluorescence images were recorded by confocal laser scanning microscopy (CLSM). The co-loaded hydrophilic dye RB was used to observe the release of Cl^- on account of they both aggregated in the hydrophilic cavity of SPN and the hydrophobic dye NA was concentrated in the shell of SPN which can indicate whether the nanocarrier enter cells. As shown in Fig. S2 (Supporting information), when the cells were incubated with dye-SPN@PDA for 1 h, the green fluorescence of hydrophobic NA was mainly observed indicating the nanocarrier entered the cells through endocytosis (Fig. S2a). After the incubation for 2 h, the bright red color was observed in cells (Fig. S2f), and the intensity of

red fluorescence became stronger with the increase of incubation time and reached a stable state at 6 h (Figs. S2g and h). In addition, the green fluorescence intensity also enhanced with the increase of time as NA becomes more dispersed after the nanocarrier collapsed (Figs. S2c and d). Furthermore, a commercial probe (MQAE) for detecting intracellular Cl^- concentration was used to observe Cl^- concentration and the fluorescence intensity of MQAE decreases with the increases of intracellular Cl^- concentration. When HeLa cells were incubated with SPN@PDA for 1, 2, 4 and 6 h, the fluorescence of MQAE gradually weakened compared with the group treated with salt-free nanocarrier NP@PDA (Fig. S3 in Supporting information), which indicated the intracellular Cl^- concentration of cells treated with SPN@PDA was increased. These images confirmed that Cl^- and Na^+ can be released into cells quickly, and provides a considerable-much basis for further study of the physiological effect of dysregulation of ions in cells.

As the incubation time increases, the morphology of the cells treated with SPN@PDA is gradually deteriorated in the bright field and there were obvious granular protrusions named apoptosis body were observed (Fig. S4 in Supporting information). This phenomenon motivated us to explore whether SPN@PDA has a similar effect with small molecule transporter which facilitates Cl^- and Na^+ influx to reduce cell survival [26]. Firstly, the effect of SPN@PDA on the survival ratio of three cancer cells (HeLa, HepG2, P815) were investigated. As shown in Fig. S5 (Supporting information), as the concentration of SPN@PDA increased, survival ratio of three cancer cells decreased to 30%–40%, which indicates that SPN@PDA could reduce the viability of the cancer cells. In contrast, PN@PDA has little effect on cell growth. These results demonstrate the decrease in cell viability is caused by the transport of Na^+ and Cl^- into the cells.

We further investigated whether SPN@PDA can lead to apoptosis. HeLa cells were incubated with 500 μg/mL of SPN@PDA for 12 h and then treated with a mixture of fluorescein-annexin V (FITC-annexin V) and propidium iodide (PI). When apoptosis occurs, both FITC and PI signals increase significantly [27]. As illustrated in Fig. 3A, flow cytometry analysis revealed that the cells treated with SPN@PDA displayed positive annexin V binding and PI uptake compared with control and PN@PDA groups, and apoptosis rate increased to 28%, which indicates SPN@PDA is capable to induce apoptosis. JC-1 (a commercial mitochondrial membrane potential staining reagent) was used for staining experiments. When mitochondrial membrane potential is normal, JC-1 is mainly in the aggregated state and red fluorescence is emitted, when apoptosis occurs, the mitochondrial membrane potential decreases, JC-1 is mainly a monomer present and green fluorescence is emitted [44]. To observe the changes of mitochondrial membrane potential, HeLa cells were treated with SPN@PDA and PN@PDA for 12 h, then stained with JC-1 and observed by CLSM. CCCP (carbonyl cyanide m-chlorophenyl- hydrazine) is a chemical reagent which induces cell mitochondrial membrane potential decline, acting as a positive control. As demonstrated in Fig. 3B, the cells treated with SPN@PDA and CCCP enhanced the green fluorescence and decreased the red fluorescence. On the contrary, PN@PDA group had little change in fluorescence signal compared with the untreated group. To further confirm SPN@PDA

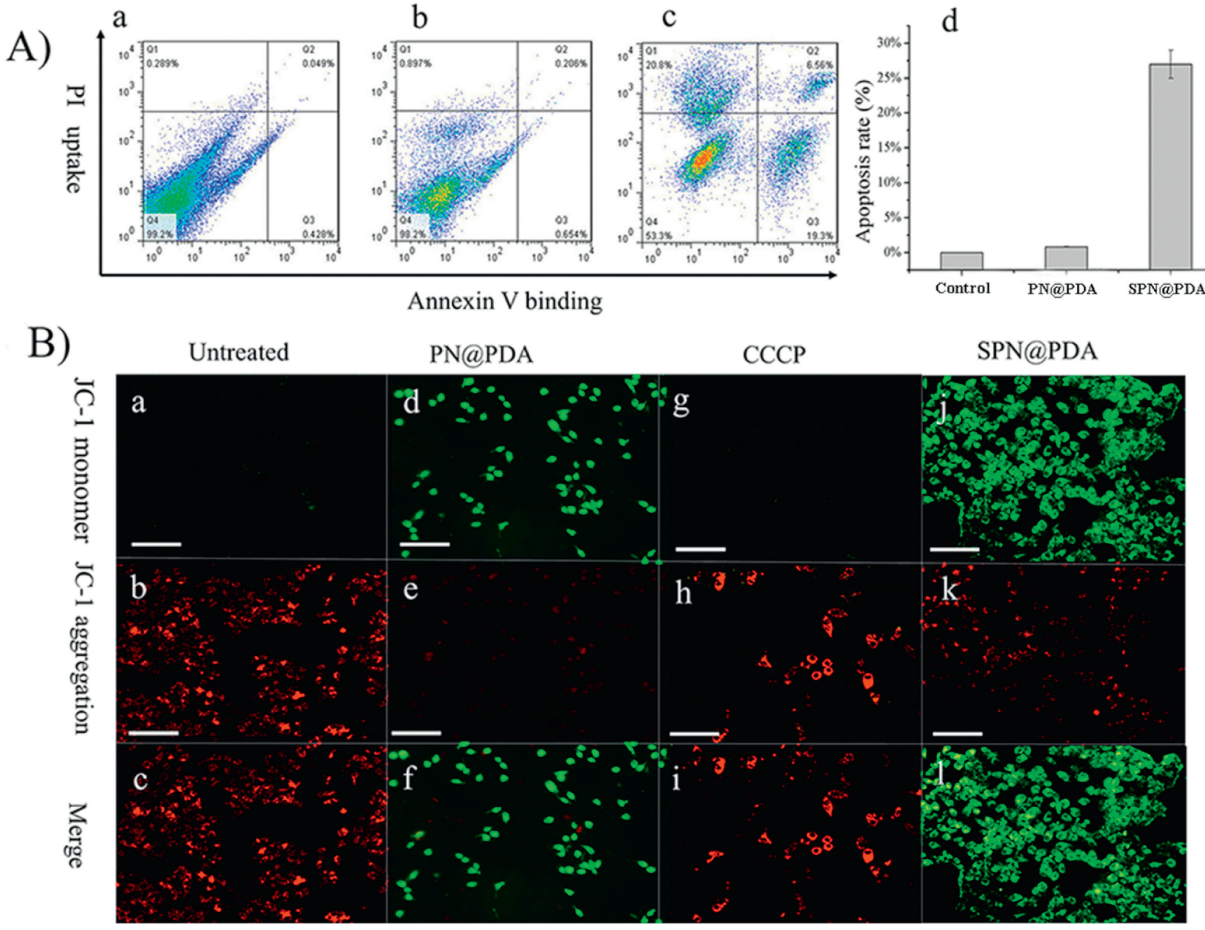

Fig. 3. (A) Flow cytometry of HeLa cells treated with PBS (a), PN@PDA (b) and SPN@PDA (c) for 12 h and stained with fluorescein-annexin V and PI (annexin V binding *versus* PI uptake), apoptosis rate histogram (d) of a, b and c. (B) HeLa cells were pretreated with PN@PDA and SPN@PDA for 12 h and stained with JC-1. Untreated cells are shown as a negative control (a–c), cells treated with CCCP are shown as positive control (d–f), PN@PDA group (g–i) and SPN@PDA group (j–l). Scale bars =100 μm.

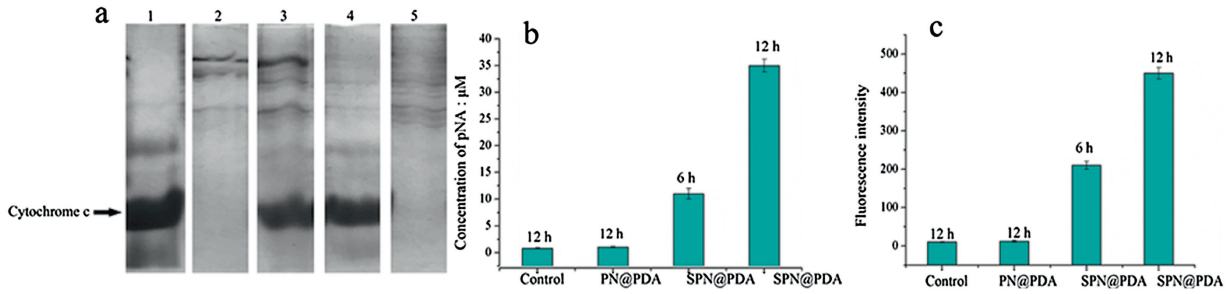

Fig. 4. (a) Determination of cytochrome c by SDS-PAGE protein electrophoresis, line 1 is the cytochrome c standard, line 2 and line 3 represent the mitochondrial and cytoplasmic extract treated with SPN@PDA correspondingly, line 4 and line 5 are mitochondrial and cytoplasmic extract of untreated cells correspondingly. (b) Concentration of pNA produced in different groups of cells lysates. (c) Fluorescence intensity of different groups of cell lysates after reacting with Ac-DEVD-AMC. $N = 3$.

can induce apoptosis, Hoechst 33258 (a commercial reagent to stain the nuclei of cells) and TUNEL (tdT-mediated dUTP nick-end labeling) staining were performed, and the detail discussions and figures (Figs. S6 and S7 in Supporting information) were shown in supporting information. All the above findings provide enough support for the fact that the SPN@PDA has apoptosis-inducing activity and the reason for inducing apoptosis with SPN@PDA should be the function of Cl^- and Na^+ releasing in cells. We also found intracellular reactive oxygen species (ROS) concentration increases when apoptosis occurs and the detail is shown in supporting information (Fig. S8 in Supporting information).

Apoptotic cell death takes place mainly via caspase dependent or independent mechanisms, and the apoptosis promoted by ion homeostasis is usually caspase-dependent [45,46]. In the caspase-dependent apoptosis pathway, mitochondria will release cytochrome c to cytoplasm, the activities of caspase-9 and caspase-3 will increase [47]. To test whether SPN@PDA induce caspase-dependent apoptosis, the following experiments were performed. Firstly, the concentrations of cytochrome c in mitochondria and cytoplasm were detected by sodium dodecyl sulfate -polyacrylamide gel electrophoresis (SDS-PAGE) protein electrophoresis. As shown in Fig. 4a, the cytochrome c in mitochondria of untreated cells is higher than in corresponding cytoplasm. In contrast, the band of cytochrome c in mitochondrial extract of cells treated with SPN@PDA is significantly lower than in corresponding cytoplasm, which illustrated cytochrome c in mitochondrial is released in cytoplasm. Then the activity of caspase-9 is detected by a substrate acetyl-Leu-Glu-His-Asp p-nitroanilide (Ac-LEHD-pNA). Caspase-9 can catalyze Ac-LEHD-pNA to produce pNA (*p*-nitroaniline) which has strong absorption at 405 nm, so the activity of caspase-9 can be determined by the absorption at 405 nm of cell lysate. In Fig. 4b, the concentration of different groups is calculated by concentration curve of pNA standard (Fig. S9 in Supporting information), and the concentrations of pNA in SPN@PDA groups (6 h and 12 h) are higher than in the control and PN@PDA groups, which means the caspase-9 activities of SPN@PDA groups are increased. Furtherly, caspase-3 activities of the treated cell lysates were then determined by using a fluorescent peptide substrate (Ac-DEVD-AMC) for caspase-3. The fluorescence intensity of Ac-DEVD-AMC increased with the increasing activity of caspase-3. It was found that the fluorescence intensity heightened with the increase incubation time of SPN@PDA compared with untreated and PN@PDA groups (Fig. 4c), which demonstrates the enhancement of caspase-3 activity. These results provide the evidence for that SPN@PDA induces apoptosis *via* a caspase-dependent pathway.

In summary, we developed a universal nanocarrier-based strategy for the delivery of ions to cells through a biocompatible and degradable polymer PLGA. Loading of $NaHCO_3$ and coating with PDA of the nanocarrier achieved the rapid release of ions, and cells apoptosis experiments verified that the Cl^- and Na^+ released from the nanocarrier promotes apoptosis when the intracellular ions balance is destroyed. The explorations of cytochrome c concentrations, caspase-9 and caspase-3 activities demonstrate the apoptosis pathway is caspase-dependent. The strategy of ions loading into biodegradable and biocompatible nanomaterials provides a novel and effective method for ions transport. Through this way, various biomaterials can be utilized to delivery all kinds of ions to target physiological environment for special therapy, even using inorganic salts to eliminate cancer cells. This is only in the preliminary exploration stage of the physiological changes caused by ion imbalance, we will try to investigate the difference between the normal cells and cancer cells in detail in the future work.

Acknowledgment

This research was financially supported by the National Natural Science Foundation of China (No. 21575055).

Appendix A. Supplementary data

Supplementary material related to this article can be found, in the online version, at doi:https://doi.org/10.1016/j.cclet.2019.09.010.

References

[1] R.M. Duke, E.B. Veale, F.M. Pfeffer, et al., Chem. Soc. Rev. 39 (2010) 3936–3953.
[2] P. Molina, F. Zapata, A. Caballero, Chem. Rev. 117 (2017) 9907–9972.
[3] J.J. Cai, J.L. Sessler, Chem. Soc. Rev. 43 (2014) 6198–6213.
[4] K. Majerski, B. Nikola, B.B. Vesna, Coord. Chem. Rev. 295 (2015) 80–124.
[5] X.N. Kan, H. Liu, Q.Y. Pan, Z.B. Li, Y.J. Zhao, Chin. Chem. Lett. 29 (2018) 261–266.
[6] E.N.W. Howe, N. Busschaert, X. Wu, et al., J. Am. Chem. Soc. 138 (2016) 8301–8308.
[7] P.A. Gale, P.T. Ricardo, R. Quesada, Acc. Chem. Res. 46 (2013) 2801–2813.
[8] Y. Okada, M.R. Blatt, G. Thiel, J. Membr. Biol. 209 (2006) 21–29.
[9] D.D. Newmeyer, M.S. Ferguson, Cell 112 (2003) 481–490.
[10] Arcangeli, B. Andrea, Curr. Med. Chem. 16 (2009) 66–93.
[11] V. Lehen'kyi, G. Shapovalov, R. Skryma, N. Prevarskaya, Am. J. Physiol. Cell Physiol. 301 (2011) C1281–C1289.
[12] S.P. Yu, L.M.T. Canzoniero, D.W. Choi, Curr. Opin. Cell Biol. 13 (2001) 405–411.
[13] B.R. Haas, V.A. Cuddapah, S.K. Watkins, et al., Am. J. Physiol. Cell Physiol. 301 (2011) C1150–C1160.
[14] A. Litan, S.A. Langhans, Front. Cell. Neurosci. 9 (2015) 86.
[15] J.P. Adelman, C.T. Bond, M. Pessia, J. Mayliet, Neuron 15 (1995) 1449–1454.
[16] T. Stauber, T.J. Jentsch, Annu. Rev. Physiol. 75 (2013) 453–477.
[17] A. Becchetti, Am. J. Physiol., Cell Physiol. 301 (2011) C255–C265.
[18] V.A. Cuddapah, H. Sontheimer, Am. J. Physiol. Cell Physiol. 301 (2011) C541–C549.
[19] W. Lin, T.Y. Cen, S.P. Wang, et al., Chin. Chem. Lett. 29 (2018) 1372–1374.
[20] N. Busschaert, C. Caltagirone, W.V. Rossom, et al., Chem. Rev. 115 (2015) 8038–8155.
[21] X. Wu, E.N.W. Howe, P.A. Gale, Acc. Chem. Res. 51 (2018) 1870–1879.
[22] N. Busschaert, P.A. Gale, Angew. Chem. Int. Ed. 52 (2013) 1374–1382.
[23] G.W. Gokel, S. Negin, Acc. Chem. Res. 46 (2013) 2824–2833.
[24] N. Busschaert, I.L. Kirby, S. Young, et al., Angew. Chem. 124 (2012) 4502–4506.
[25] J. Yang, C.C. Dong, X.L. Chen, et al., J. Am. Chem. Soc. 141 (2019) 4597–4612.
[26] S.K. Ko, S.K. Kim, A.V. Share, et al., Nat. Chem. 6 (2014) 6885–6892.
[27] N. Busschaert, S.H. Park, K.H. Baek, et al., Nat. Chem. 9 (2017) 667–675.
[28] E.M. Cohen, H.Y. Ding, C.W. Kessinger, et al., Otolaryng. Head Neck 143 (2010) 109–115.
[29] M.N. Wang, A.M. Mihut, E. Rieloff, et al., PNAS 116 (2019) 5442–5450.

[30] L. Tao, W. Hu, Y.L. Liu, et al., Exp. Bio. Med. 236 (2011) 20–29.
[31] W. Tao, X.W. Zeng, T. Liu, Acta Biomater. 9 (2013) 8910–8920.
[32] J. Nicolas, S. Mura, D. Brambilla, N. Mackiewicz, P. Couvreur, Chem. Soc. Rev. 42 (2013) 1147–1235.
[33] E.C. Dreaden, A.M. Alkilany, X. Huang, C.J. Murphy, M.A. El-Sayed, Chem. Soc. Rev. 41 (2012) 2740–2779.
[34] W.H. Jia, T.L. Zhang, Z.G. Lu, et al., Chin. Chem. Lett. 30 (2019) 739–742.
[35] C.J. Ke, T.Y. Su, H.L. Chen, et al., Angew. Chem. Int. Ed. 50 (2011) 8286-8239.
[36] X. Liang, Y. Yang, L.J. Wang, et al., J. Mater. Chem. B 3 (2015) 9383–9386.
[37] M.H. Li, X.T. Sun, N. Zhang, et al., Adv. Sci. 5 (2018) 1800155.
[38] L. Ding, X.B. Zhu, Y.L. Wang, et al., Nano Lett. 17 (2017) 6790–6801.
[39] Y.Y. Li, C.H. Jiang, D.W. Zhang, et al., Acta Biomater. 47 (2017) 124–134.
[40] Yang Li, X.L. Wang, D.W. Yang, et al., J. Mater. Sci. 54 (2019) 12036–12048.
[41] J. Park, Y.H. Pei, H. Hyun, et al., J. Control. Release 268 (2017) 407–415.
[42] Y.P. Ding, S.S. Su, R.R. Zhang, et al., Biomaterials 113 (2017) 243–252.
[43] M. Zhang, R.X. Song, Y.Y. Liu, et al., Chemistry 5 (2019) 1–12.
[44] S.K. Ko, I. Shin, ChemBioChem 13 (2012) 1483–1489.
[45] M. Tsukimoto, H. Harada, A. Ikari, J. Biol. Chem. 280 (2005) 2653–2658.
[46] Z. Hu, H.P. Xing, Z. Zhu, W. Wang, W.C. Guan, Chin. Chem. Lett. 18 (2007) 145–148.
[47] P. Li, D. Nijhawan, I. Budihardjo, et al., Cell 91 (1997) 479–489.